Bio-based monomers for UV-curable coatings: allylation of ferulic acid and investigation of photocured thiol-ene network

Bio-based Monomers for UV-Curable Coatings:

Allylation of Ferulic acid and Investigation of Photocured Thiol-ene Network

L. Pezzana[a], M. Mousa[b], E. Malmström[b,c], M. Johansson*[,b,c], M. Sangermano*[,a]

[a] Politecnico di Torino, Department of Applied Science and Technology, Corso Duca degli Abruzzi 24, 10129 Torino, Italy

[b] KTH Royal Institute of Technology, School of Engineering Sciences in Chemistry, Biotechnology and Health, Department of Fibre and Polymer Technology, Teknikringen 56–58, SE-100 44 Stockholm, Sweden

[c] Wallenberg Wood Science Centre, Teknikringen 56-58, SE-100 44 Stockholm, Sweden

* Corresponding authors

Keywords: UV-curable coatings, bio-based monomer, ferulic acid, thiol-ene

Abstract: Ferulic acid (FA) is an unsaturated hydroxycinnamic acid that can be isolated from lignin. In this study, the biorenewable FA was allylated to result in a library of mono- or diallylated monomers, either having the inherent cinnamoyl~~allylic~~ double bond intact or saturated through hydrogenolysis. All monomers were photo-chemically cured with trimethylolpropane tris(3-mercaptopropionate) (TRIS) into crosslinked films in the presence of a photoinitiator (Irgacue 819). The reactivity of the FA-derived monomers toward TRIS was investigated in detail by photorheology and FT-IR spectroscopy to reveal details on the relative reaction rates for the different alkene groups~~.~~. The thermo-mechanical properties of the crosslinked films were fully characterized by means of dynamic mechanical analysis (DMTA) and thermal calorimetry (DSC). It was demonstrated that the glass transition temperature of the final crosslinked network could be controlled by the addition of a monoallylated monomer. By increasing the content of the monoallylated compound, it was possible to observe a linear decrease of the Tg-values of the crosslinked films.

Corresponding authors*:

matskg@kth.se

marco.sangermano@polito.it

1. INTRODUCTION

Polymer scientists and industry are facing a challenging shift from fossil-based to bio-based materials; by the end of the next decade, many current petroleum-derived products should be replaced by less expensive and better-performing products based on renewable materials [1]. In literature, different renewable monomers are explored as precursors to polymers such as sugars, polysaccharides, vegetable oils, lignin, pine resin derivatives, and proteins [2]–[4]. Among them ferulic acid, Figure 1, shows significant potential owing to its chemical structure and abundance. Ferulic acid, or (E)-3-(4-hydroxy-3-methoxyphenyl) prop-2-enoicacid, is a naturally occurring trans-cinnamic acid derivative (HCAs) [5] discovered in 1866 as a component of *Ferula foetida* Reg. (*Umbelliferae*). Its name, ferulic acid (FA), is derived from the plant from which it is extracted [6]. FA belongs to the *p*-hydroxycinnamic family together with caffeic acid and sinapic acid, Figure 1. FA is a multifunctional compound, having three functional groups; a phenol, a cinnamoyl double bond, and a carboxylic acid-group.

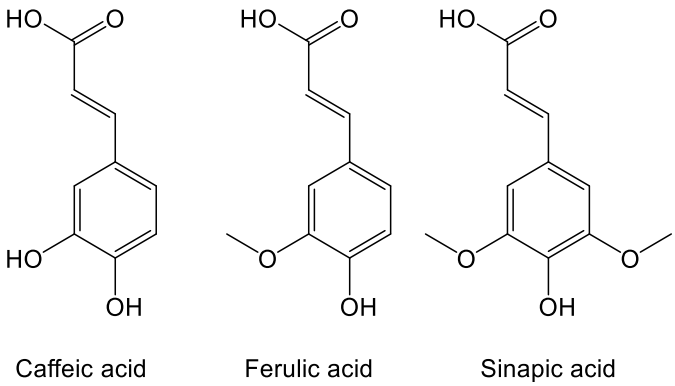

Figure 1: Chemical structures of three *p*-hydroxycinnamic acids; caffeic acid (left), ferulic acid (FA, middle), and sinapic acid (right).

FA is a component in lignin, the second most abundant biopolymer (after cellulose) on Earth, representing 30 % of the organic carbon in the biosphere [7]. Lignin can be obtained as a by-product from the pulp and paper industry, or from the production of food from crops and cereals, and is therefore readily abundant and hence, a ~~realistic~~ scalable source of FA [8]. FA is usually concentrated in the bran of grains, peel of fruits, roots and peel of vegetables. In maize for example, the FA content is around 3-4 % of the dry weight [9]. FA is produced according to the phenylpropanoid pathway, it couples oxidatively to other FAs and FA-derivatives, lignin, and structural proteins within the cell wall. The links to lignin and proteins by ether bonds and to polysaccharides by ester bonds, act as universal connectors between cell wall polymers. FA has a key role in cessation of cell growth, anchoring lignin to cell wall polysaccharides, restricting the accessibility of plant pathogens. It influences properties such as adherence, extensibility, accessibility and biodegradability. FA plays an important role in the production of cellulosic ethanol, that is becoming an important supply for the fuel industry [10].

FA has been explored for a range of properties; as antioxidant, for anti-allergenic, anti-inflammatory, and antimicrobial purposes. It has been proposed to be used as an anticancer agent and, since it can absorb UV-light, in cosmetics to protect the skin [11], [12].

FA has attracted interest by polymer chemists and has been evaluated as a promising bio-renewable monomer to substitute some of the fossil-based monomers already used, for instance in poly(ethylene

terephthalate) (PET) [13]. In this potential application, FA is converted into a polyester but it can also be an interesting starting building block for polyurethanes, epoxides and phenolic resins as well [14]. FA provides versatile handles for further chemistries as the phenolic and carboxylic groups can be exploited for further functionalization. FA is particularly interesting as it is one of few biorenewable aromatic compounds that contain a double bond and may therefor find use in chain-wise polymerization, to replace meth(acrylates). The double bond can potentially be employed in photo-initiated (UV) polymerizations (i.e. radiation curing).

Radiation curing is attracting increasing interest especially in the field of coatings, as witnessed by the large number of books and review articles published in the last 20 years [15]–[23]. UV-curing shows important advantages such as high-speed cure, reduced energy consumption and absence of VOC emission as many systems are low viscous, without the need of any solvents. Among the different UV-curing processes, thiol-ene photopolymerization is attracting attention due to its "click" characteristics implying that very high conversions are reached [15], [17], [18]. The rationale for using free-radical thiol-ene polymerization is that it allows for ene-monomers that normally do not homopolymerize to be employed as comonomers in conjunction with the thiols. This is especially important when searching for bio-based unsaturated monomers which generally are di- or trisubstituted and hence rather challenging to homopolymerize due to steric reasons. Free-radical thiol-ene reactions have, for example, been demonstrated for unsaturated vegetable oils (1,2-disubstituted alkenes) [24], [25], terpenes (1,1,2-trisubstituted and 1,1-disubstituted alkenes) [26]–[28], and unsaturated lignin–derivatives [29].

The reaction rate for differently substituted alkenes in a thiol-ene reaction strongly depends on the substitution pattern of the alkene, as for example presented by Hoyle [30]. This has to be taken into account when ~~different~~ several alkenes are present in a curing system and can also be employed as a tool to design thermoset structures, as described by Bowman *et al*. for ternary monomer systems [31], [32]. It should, however, in general be noted that enes that are less prone to homopolymerize provide more of a "click"-character to thiol-ene reaction compared to readily homopolymerizable monomers e.g. acrylates. The allyl ether-functionality utilized in the present study is very slow in free radical homopolymerization compared to acrylates and is thus very well suited for thiol-ene reactions [18]. Allylation of caffeic acid and other bio-based monomers has already been proposed in literature as a pathway to a new precursor platform for photo-curable biorenewable thermosets [33], [34].

In this paper, we report the allylation of FA~~,~~ to achieve ~~either~~ mono- or bifunctional allyl monomers, and their use in UV-initiated thiol-ene polymerization. The reactivity of the bio-renewable monomers towards trimethylolpropane tris(3-mercaptopropionate) was investigated in detail~~,~~ by photorheology and FT-IR analysis. The thermo-mechanical properties of crosslinked films were fully characterized by means of DMTA and DSC analysis. Finally, the influence of the addition of monoallyl-functional FA-derived monomers on kinetics and the properties of the crosslinked films were investigated.

2. EXPERIMENTAL

2.1 Materials

Ferulic acid (FA) was supplied by Sigma-Aldrich and used as received. Allyl bromide, sodium hydroxide (NaOH), potassium carbonate (K_2CO_3), Pd (10 % on activated carbon) were obtained from Sigma-Aldrich. $MgSO_4$ was provided by Acros Organic. Acetone and methanol (MeOH), ethyl acetate (EtOAc) were supplied by VWR Chemicals and dichloromethane (DCM) from Merck KGaA. Hydrochloric acid, (HCl 37 %) and sulphuric acid (H_2SO_4, 95 %) were supplied by VWR Solvent. NMR analysis was performed with either deuterated chloroform, $CDCl_3$, or dimethyl sulfoxide, DMSO-d_6 provided by VWR Chemicals. The trimethylolpropane tris(3-mercaptopropionate), TRIS, was supplied by Bruno Bock Gmbh and the photoinitiator Irgacure 819 was provided by BASF.

2.2 Monomers synthesis

Diallylated derivative of ferulic acid (A2FA).

FA (2.08 g, 10.7 mmol) and potassium carbonate (5.91 g, 42.8 mmol) were placed in a two-neck round-bottomed flask and dissolved in acetone (40 mL). The mixture was stirred to allow the dissolution of FA where after allyl bromide (2.35 mL, 26.7 mmol) was added. The reaction was then kept at reflux (~55 °C) for about 20 hours. Then the mixture was filtered, and the solvent was evaporated. The crude product was dissolved in DCM (20 mL) and extracted with water. The water phase was extracted three times with DCM then the organic fractions layers were combined and dried over $MgSO_4$ to obtain give the product. Finally, the solvent was removed under reduced pressure on a rotavapor. The A2FA was used without further purification.
Yellow-orange liquid, 2.39 g, 82 % yield. ^{1}H NMR (400 MHz, DMSO-d_6) δ = 7.61 (d, *J* = 15.9 Hz, 1H), 7.37 (d, *J* = 2.0 Hz, 1H), 7.21 (dd, *J* = 8.3, 1.9 Hz, 1H), 6.97 (d, *J* = 8.3 Hz, 1H), 6.58 (d, *J* = 15.9 Hz, 1H), 6.01 (dddt, *J* = 20.9, 17.4, 10.6, 5.4 Hz, 2H), 5.43 – 5.20 (m, 4H), 4.63 (ddt, *J* = 29.3, 5.4, 1.5 Hz, 4H), 3.82 (s, 3H) ppm. ^{13}C NMR (101 MHz, DMSO-d_6) δ = 166.10, 149.82, 149.17, 144.88, 133.42, 132.84, 127.02, 122.78, 117.75, 117.70, 115.34, 112.89, 110.70, 68.81, 64.30, 55.64 ppm.

Hydrogenated ferulic acid (h-FA)

FA (20 g, 103 mmol) was dissolved in MeOH (100 mL) under stirring. Pd on activated carbon (2 g) was added to a round-bottomed flask. The flask was sealed with a septum and argon was applied to degas the reaction flask. The FA-solution was added to the flask with a syringe where after H_2 (g) was applied using a H_2-balloon. The mixture was stirred 24 hours at room temperature then the Pd/C was filtered off through a glass filter (NS 5). The solvent was then evaporated using a rotavapor to obtain the product as a whitish powder, 19.2 g, 95 % yield. ^{1}H NMR (400 MHz, $CDCl_3$) δ = 6.86 – 6.70 (m, 3H), 3.87 (s, 3H), 2.89 (t, *J* = 7.7 Hz, 2H), 2.66 (t, *J* = 7.7 Hz, 2H) ppm. ^{13}C NMR (101 MHz, $CDCl_3$) δ = 178.95, 146.59, 144.25, 132.21, 120.99, 114.55, 111.07, 56.02, 36.10, 30.49 ppm.

Synthesis of diallylated hydrogenated derivative of ferulic acid (h-A2FA)

h-FA (3.22 g, 16.4 mmol) and potassium carbonate (9.10 g, 65.7 mmol) were added to a two-neck round-bottomed flask and dissolved in acetone (~50 mL). The mixture was stirred to allow the dissolution of h-FA where after allyl bromide (3.45 mL, 39.4 mmol) was added. The reaction was then left for 24 hours under reflux. Then the mixture was filtered, the solvent was evaporated, and extraction with DCM was performed. The water layer was extracted three times with DCM, then the combined organic phase was dried using $MgSO_4$. Finally, evaporation of the solvent was performed with rotavapor. The h-A2FA was used without further purification.
Yellow liquid, 4.24 g, 93 % yield. ^{1}H NMR (400 MHz, $CDCl_3$) δ = 6.80 (d, *J* = 8.1 Hz, 1H), 6.75 – 6.65 (m, 2H), 6.07 (ddt, *J* = 17.4, 10.6, 5.4 Hz, 1H), 5.90 (ddt, *J* = 17.3, 10.5, 5.7 Hz, 1H), 5.44 – 5.18 (m, 4H), 4.58 (dq, *J* = 5.7, 1.4 Hz, 4H), 3.86 (s, 3H), 2.91 (t, *J* = 7.7 Hz, 2H), 2.64 (dd, *J* = 8.4, 7.1 Hz, 2H) ppm. ^{13}C NMR (101 MHz, $CDCl_3$) δ = 172.58, 149.39, 146.47, 133.53, 133.51, 132.16, 120.07, 118.22, 117.83, 113.65, 112.06, 70.00, 65.13, 55.89, 36.10, 30.59 ppm.

Monoallylated hydrogenated derivative of ferulic acid (h-A1FA).

h-FA (3.33 g, 17.0 mmol) was dissolved in acetone (50 mL). K_2CO_3 (9.38 g, 67.8 mmol) was added and then allyl bromide (3.55 mL, 40.7 mmol) was added using a micropipette. The mixture was kept at reflux for 24 hours under vigorous stirring. After cooling, the solution was filtered, and the solvent was removed under reduced pressure. The residue was dissolved in a mixture of NaOH (aq) (75 mL, 2 M) and EtOH (50 mL), then the solution was heated to reflux for 2 hours. After cooling, the solvent was partially evaporated. Then HCl (6 M) was added dropwise to precipitate the product. The product was filtrated filtered and dried in a vacuum oven over night.

Yellowish powder, 3.~~,~~85 g, 96 % yield. ^{1}H NMR (400 MHz, $CDCl_3$) δ = 10.67 (s, 1H), 6.83 (d, *J* = 8.1 Hz, 1H), 6.79 – 6.70 (m, 2H), 6.10 (ddt, *J* = 16.2, 10.6, 5.4 Hz, 1H), 5.46 – 5.37 (m, 1H), 5.33 – 5.25 (m, 1H), 4.61 (d, *J* = 5.4 Hz, 2H), 3.88 (s, 3H), 2.93 (t, *J* = 7.7 Hz, 2H), 2.69 (t, *J* = 7.7 Hz, 2H) ppm. ^{13}C NMR (101 MHz, $CDCl_3$) δ = 178.94, 149.41, 146.55, 133.48, 133.17, 120.03, 117.87, 113.66, 112.06, 69.99, 55.90, 35.81, 30.25 ppm.

Methyl ester of allylated hydrogenated ferulic acid (h-EA1FA)

h-A1FA (2.0 g, 8.5 mmol) was dissolved in MeOH (40 mL) where after H_2SO_4 was added in a catalytic amount. The solution was refluxed 24 hours. After cooling, the product was extracted with EtOAc. The organic layers were combined and washed with ~~saturated solutions~~ portions of saturated $NaHCO_3$ and brine, respectively, and dried over $MgSO_4$. Finally, the solvent was evaporated on a rotavapor.
Orange-brown liquid, 1.99 g, 94 % yield. ^{1}H NMR (400 MHz, $CDCl_3$) δ = 6.79 (dd, *J* = 8.1, 1.9 Hz, 1H), 6.74 – 6.66 (m, 2H), 6.07 (dddd, *J* = 15.9, 12.7, 6.5, 4.4 Hz, 1H), 5.43 – 5.20 (m, 2H), 4.57 (ddt, *J* = 5.4, 2.8, 1.5 Hz, 2H), 3.85 (d, *J* = 2.1 Hz, 3H), 3.66 (d, *J* = 2.5 Hz, 3H), 2.89 (td, *J* = 7.7, 1.8 Hz, 2H), 2.60 (td, *J* = 7.9, 1.8 Hz, 2H) ppm. ^{13}C NMR (101 MHz, $CDCl_3$) δ = 173.48, 149.49, 146.57, 133.65, 120.14, 117.92, 113.75, 112.15, 70.09, 55.99, 51.70, 36.06, 30.71 ppm.

2.3 Photopolymerization

The synthesized allylated-monomers, Scheme 1, were evaluated in a series of different photocurable formulations, Table 1. Trimethylolpropane tris(3-mercaptopropionate) (TRIS) was used as thiol-functional crosslinker in all formulations. ~~The formulations were prepared according to Table 1~~. Most ~~photocurable formulations~~ mixtures were prepared by adding stoichiometric amounts of thiols and enes (1:1 molar ratio). A2FA was, however, used in two different ratios, ~~where the thiol-crosslinker was added~~ either in a 1:1 molar ratio thiol:allyl ether, or 1:1 molar ratio thiol:total enes. ~~The amount of photoinitiator added in each formulation was 0.5 wt-% of the total of mass of the resins~~. The photoinitiator used was Irgacure 819 in accordance to previous works [16], [17] and used in 0.5 wt-% of the total of mass of the resin.

The photocurable formulation were prepared using the following procedure as exemplified by entry 3 in Table 1. A2FA (200 mg) was placed in a test tube together with h-EA1FA (10 mg) and then TRIS (204 mg) was added. The test tube was stirred for 5 min in an ultrasonic bath. The photoinitiator, Irgacure 819 (2 mg), was finally added whereafter the test tube was covered with aluminum foil and stirred for another 2-3 min to ensure a complete dissolution. A set of films was prepared using a silicon mold (~~each films had these average dimensions,~~ 8 x 12 mm, and the thickness was 0.1 mm, 0.2 mm, 0.3 mm, 0.4 mm, and 0.6 mm respectively). The UV irradiation was performed with a Dymax ECE 5000 Flood lamp. The irradiation time was 1 or 2 minutes (~~110~~ _mW/cm^2).

Table 1: Summary of the prepared photocurable formulations. Trimethylolpropane tris(3-mercaptopropionate) (TRIS) was used as a crosslinking trithiol and Irgacure 819 (0.5 wt-%) as a photoinitiator in all formulations.

Entry	**Molar ratio thiol : ene 1:1**	**Diallylated monomers**		**Monoallylated monomer h-EA1FA(1) (mg)**	**Thiol TRIS (mg)**
		A2FA (mg)	**h-A2FA (mg)**		
1	thiol : allyl ether	215	-	-	208
2	thiol : total ene	195	-	-	283

3	thiol : allyl ether	200	-	10 (5 %)	199
4	thiol : allyl ether	204	-	21 (10 %)	209
5	thiol : allyl ether	207	-	33 (15 %)	218
6	thiol : allyl ether	-	220	-	212
7	thiol : allyl ether	-	216	10 (5 %)	213
8	thiol : allyl ether	-	222	22 (10 %)	225
9	thiol : allyl ether	-	209	33 (15 %)	219

(1) Added in molar amount 5%, 10% or 15% relative to the diallylated monomer

2.4 Characterization

2.4.1 Nuclear magnetic resonance (NMR)

NMR was conducted on a Bruker AM 400. ^{1}H-NMR and ^{13}C-NMR spectra were recorded at 400 MHz and 101 MHz respectively. Either $CDCl_3$ or DMSO-d_6 was used as solvent.

2.4.2 Photorheology

An~~The instrument~~ Anton Paar MC 302 rheometer was used for the photorheology measurements. The light source was a~~from~~ Hamamatsu LIGHTINGCURE LC8~~ was~~ equipped with an optic fiber. The intensity of the UV light was 30 mW/cm^2. The conditions for the tests were the following: frequency of 1 Hz, strain of 1 %, the lamp was switched on after 30 seconds. The rheometer was set as a plate-plate, the accessory had a diameter of 2.5 cm. The distance between the crystal and the plate was 200 µm which corresponds approximately to 150 µL of coating resin.

2.4.3 UV-vis spectroscopy

The measurement was done with a Jenway 6850 UV/Vis. Spectrophotometer. The spectra were recorded from 450 ηm to 200 ηm. Quartz cuvettes were used. DCM was used as solvent, and the concentration of the two different monomers was 0.03 mg/L and 0.04 mg/L for A2FA and h-A2FA respectively.

2.4.4 Fourier transform infrared spectroscopy (FTIR)

The instrument used for the characterization of the different formulations was a Nicolet iS 50 Spectrometer. Data pre- and post-curing were collected as 32 scans with a spectral resolution of 4.0 cm^{-1}. All data were recorded and handled with the software Omnic from Thermo Fischer Scientific. The lamp was a Hamamatsu LIGHTINGCURE LC8 equipped with an optic fiber. Conversion curves were recorded to monitor the disappearance of the thiol-peak at 2590 cm^{-1} and the reduction of the double bond peak at 1640 cm^{-1}. The aromatic ring in the samples was assumed to be unaffected by the irradiation and the stretching of aromatic double bonds (-C=C-) at 1550 cm^{-1} was thus used as the reference peak. Equation 1 was used to calculate the final conversion.

$$Conversion = \frac{(A_{2590}/A_{1550})_{t=0} - (A_{2590}/A_{1550})_t}{(A_{2590}/A_{1550})_{t=0}} \qquad \text{equation 1}$$

2.4.5 Dynamic mechanical thermal analysis (DMTA) and evaluation of crosslinking density

The DMTA analysis was performed with a Triton Technology instrument. The following parameters were used; 3 °C/min as heating rate, starting temperature was set to -40 °C with an applied tensile stress frequency of 1 Hz. The measurements were stopped after the appearance of the plateau in the storage modulus. Liquid nitrogen was used to cool down the chamber. The analyzed samples had an average dimension of 0.4 x 8 x 12 mm.
Equation 2 is derived from the statistical theory of rubber elasticity and gives an estimation of the strand density, density of cross-links

$$\nu_c = \frac{E'}{3RT} \quad (2)$$

where ν_c is the number of crosslinks per volume of the crosslinked network, E' is the storage modulus in the rubbery plateau (Tg + 50 °C), R is the gas constant and T is the temperature in Kelvin.

2.4.6 Differential scanning calorimetry (DSC)

The DSC analysis was performed on a Mettler Toledo DSC-1 equipped with Gas Controller GC100. The method used was the follow: the starting temperature was set as 30 °C; the first heating goes from 30 to 100 °C; then the temperature was maintained at 100 °C for 2 minutes in order to stabilize the sample, after that the chamber was again cooled until -50 °C wasis reached and then this temperature was maintained for 4 min, finally was applied a second heating from -50 °C to 100 °C applied. The heating and the cooling rates were set at 10 °C/min and the analysis was performed in a nitrogen atmosphere with a flow rate 20 mL/min. In this study 40 µL aluminum pans were used. The data were analyzed with Mettler Toledo STARe software V9.2.

2.4.7. Coating properties

The contact angle measure was performed by Drop Shape Analyzer, DSA100, Krüss. The measurer reported results are was an average of conducted analyzing at least of at least 5 different water's droplets.
AnThe instrument Anton Paar MC 302 rheometer was used to measure the viscosities. The rheometer was set as a plate-plate geometry with, the accessory had a diameter of 2.5 cm. The temperature was set at 25 °C.
The pencil hardness and the adhesion were measured according the standard ASTM D3363 and ASTM D3359. For the hardness different pencil were used from 8 B to 8 H. Instead Eclometer 107, as cross hatch cutter, was used for determining the adhesion. The insert number 2 was used as cutter. The films were photocured on glass substrate.

3. RESULT AND DISCUSSION

3.1 Monomer synthesis

Ferulic acid (FA) proved to be a very suitable substrate for monomer synthesis and all monomers could be produced in high yields without significant side reactions The versatility of FA as a starting material was clearly demonstrated in the monomer synthesis (Scheme 1) where functionalities such as allyl aryl ethers, coumaryl alkenes, carboxylic acids, methyl esters, allyl esters, and phenols could

be combined in different ways. It should also be noted that all reactions proved to be very selective, resulted in high yields, and with products easy to purify using scalable techniques.

Scheme 1: Synthetic pathways used to achieve the various monomers from FA.

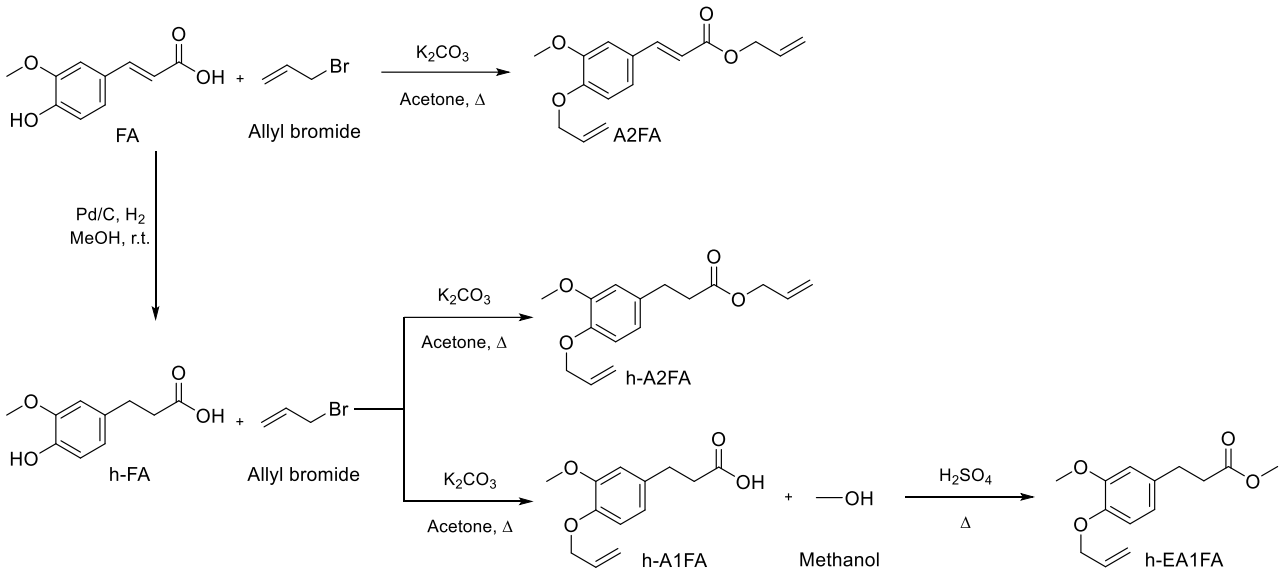

3.2 Photocuring kinetics

Allyl-functional FA-based monomers were synthesized following the methods reported in the experimental part. The monomers were fully characterized and their reactivity in thiol-ene photopolymerization was investigated, using trimethylolpropane tris(3-mercaptopropionate) as thiol-functional crosslinker in 1:1 molar ratio with respect to thiol-to-ene, Table 1, using photorheology and FTIR in the presence of Irgacure 819.

The cross-linking kinetics were investigated by photorheology and representative graphs are reported in Figure 2. When comparing the first set of samples (h-A2FA and A2FA) having a 1:1 molar ratio thiol:allyl ether it can be observed that the storage modulus for h-A2FA monomer is characterized by a steeper slope and reach a plateau value faster than the A2FA monomer. Moreover, the h-A2FA reaction started immediately when the lamp was turned on whereas the A2FA exhibited an induction time. This induction could be attributed to several reasons where one is the UV-absorption properties of the A2FA monomer. Due to its resonance structure it may compete with the absorption of the photoinitiator [35]. When the cinnamoyl double bond is removed, as in h-A2FA, the absorption is shifted to shorter wavelengths and no more UV-absorption competition occurs why a faster photo-polymerization without any induction time is observed. This hypothesis was indeed corroborated by UV-vis analyses of A2FA and h-A2FA, Figure 3.

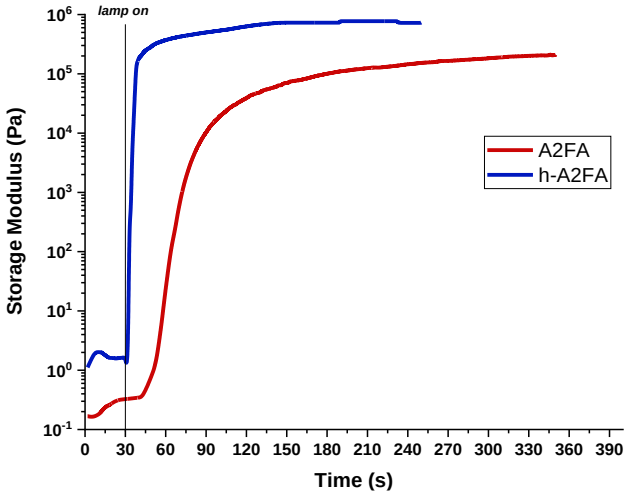

Figure 2: Photo-rheology comparison between the h-A2FA (Table 1, entry 6) and A2FA (Table 1, entry 1) formulations.

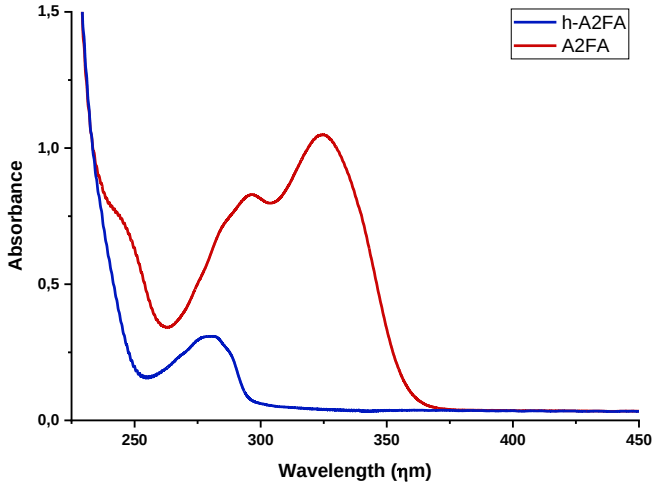

Figure 3: UV-vis spectra of A2FA (red) and h-A2FA (blue).

Scheme 2 shows a representation of the thiol-ene photocuring process, when the h-A2FA monomer was used together with TRIS. FT-IR spectroscopy was used to monitor the curing reaction by following the disappearance of the thiol- and ene-reactive groups.

Scheme 2: A schematic illustration showing the thiol-ene photopolymerization of h-A2FA and TRIS in the presence of Irgacure 819 (Table 1, entry 6).

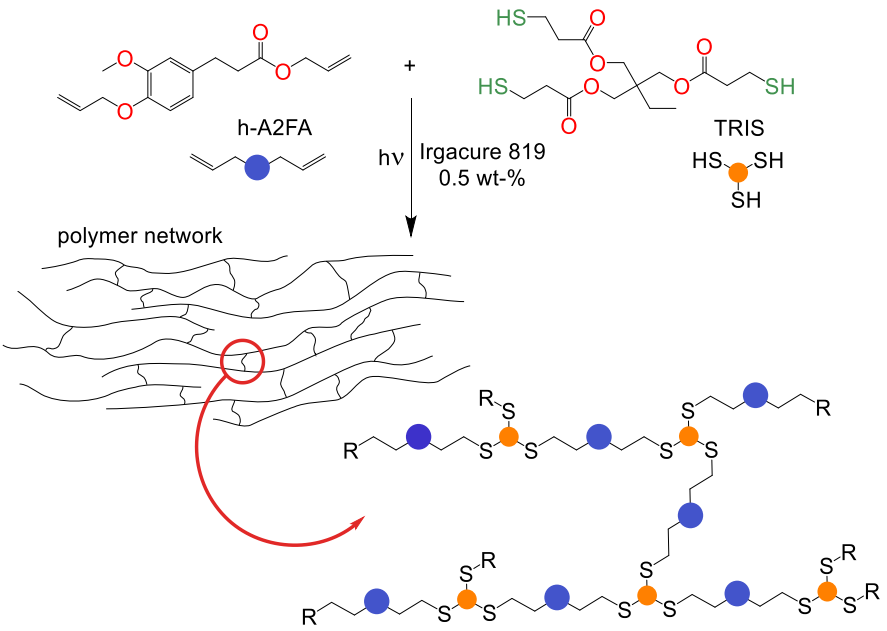

Since ~~the~~ IR absorbance is proportional to the concentration of a compound, conversion versus time profiles can be acquired, Figures 4 and 5.

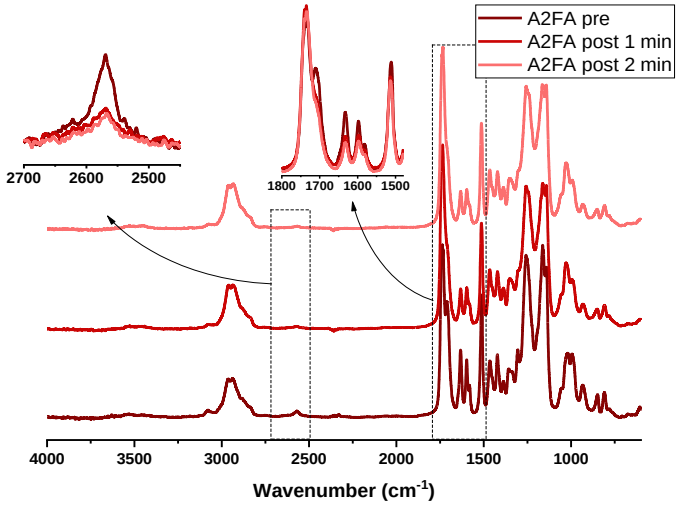

Figure 4: FTIR spectra for A2FA (Table 1, entry 1) acquired prior to irradiation and after 1 and 2 minutes of irradiation, (-SH 2590 cm^{-1}, -C=C- 1640 cm^{-1}).

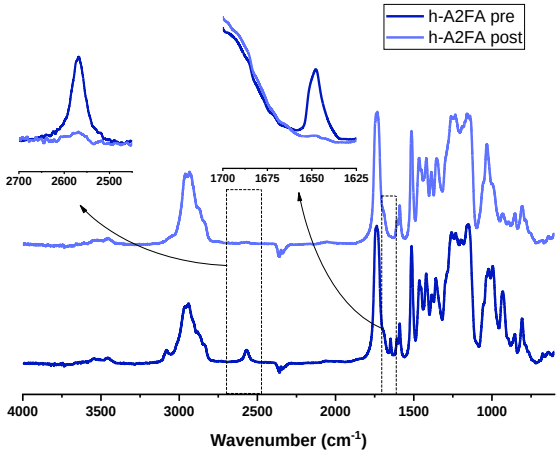

Figure 5: FTIR spectra for h-A2FA (Table 1, entry 6), -SH peak 2590 cm^{-1}, -C=C- peaks 1640 cm^{-1}.

The enlarged areas between 2500 and 2700 cm^{-1} are attributed to the thiol-group, while the peaks centered at around 1640 cm^{-1} is related to the ene (C=C) double bonds. By FT-IR analysis it is possible to evaluate the thiol-ene conversion during irradiation, Equation 1.
The h-A2FA monomer reached higher conversion than A2FA, Table 2. Both the thiol-group and the C=C double bond reached full conversion. This confirms the stochiometric reaction, typical of the thiol-ene step-growth mechanism, Figure 5.
The total conversion of A2FA was around 85 % for the thiol-group (2590 cm^{-1}), while the conversion of the double bond 1640 cm^{-1} was significantly lower, Figure 4. It is further observed that the shoulder of the carbonyl peak at 1700 cm^{-1}, which corresponds to the carbonyl group when conjugated with the cinnamoyl alkene, is strongly reduced. This implies that most of the cinnamoyl alkenes have been consumed and that it is mainly unreacted allyl ethers that remain as residual unsaturations. This suggest that the initial addition of a thiyl-radical is faster in adding to the cinnamoyl alkene than to the allyl ether and that the subsequent hydrogen abstraction of the thiol hydrogen by a carbon-centered radical is the rate-determining step. This corroborates well with the reduced slope observed in Figure 2. We also modified the thiol-content considering the A2FA-monomer as trifunctional monomer (therefore increasing the thiol molar content in the photocurable formulation) A2FA was thus evaluated in two different formulations, where the thiol-crosslinker was added either in a 1:1 molar ratio thiol:allyl ether, or 1:1 molar ratio thiol:total enes, Table 1, entries 1 and 2.The FT-IR spectra before and after 1 and 2 minutes of irradiation are reported in Figure 6. The results obtained by changing the formulation ratio shows an almost complete thiol-conversion already after 1 minute of irradiation. Moreover, the reduction of the peak related to ene double bond was more evident than in the formulation in which A2FA was evaluated as a bi-functional monomer, Figure 4.

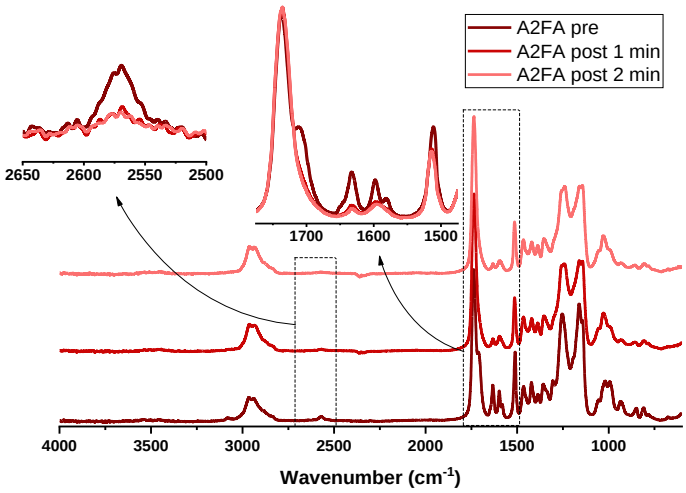

Figure 6: FTIR spectra of A2FA evaluated as a trifunctional monomer (Table 1, entry 2), -SH peak 2590 cm^{-1}, C=C peaks 1640 cm^{-1}.

3.3 Thermal and viscoelastic properties of crosslinked films

The thermal, thermomechanical and viscoelastic properties of UV-cured films were evaluated by means of DSC and DMTA analysis. DSC analysis gives information about the thermal behavior while DMTA allows the evaluation of the elastic and viscous components of the modulus of the material over a large temperature interval. Therefore, combining these techniques, a good characterization of the thermal and viscoelastic properties of the materials is obtained. The E' and tan-δ thermograms are reported in Figures 7A and 7B respectively, for the investigated photocurable formulations. All data are collected in Table 2.

The modulus above Tg recorded for the crosslinked films obtained from the A2FA-monomer, considered as a bifunctional ene-monomer, reached a lower value than the modulus registered for the crosslinked films obtained from the h-A2FA-monomer. This agrees with the photo-rheology data and with the calculated conversion previously discussed. The E' evaluated for the crosslinked films obtained by considering the monomer A2FA as trifunctional was the highest (Figure 7A). The data was in good agreement with the higher conversion calculated in the FTIR analysis when stochiometric amount of thiol was added with respect to A2FA monomer as a trifunctional ene-monomer. This can be explained with a higher number of reactive sites and final higher cross link density.

In the Tg region the tan–δ curve (tan δ = E''/E': ratio loss modulus/storage modulus) shows a maximum which is assumed as the Tg of the cured films. The crosslinked film obtained by A2FA monomer employed as bifunctional monomer, showed a Tg of about 20 °C, while the crosslinked film obtained by using the h-A2FA monomer showed a Tg of about 1 °C. The lower Tg for the h-A2FA crosslinked film, despite a higher total conversion, can be explained by the difference in the chemical structure of the monomers. In fact, while the double bond in the A2FA-structure is conjugated to the benzyl ring, increasing the network stiffness because of hindering of chain-rotation, the absence of the double bond in h-A2FA monomer, render the polymer network more flexible with a consequent decrease of the Tg-value.

The DSC thermograms for the different crosslinked formulations are reported in Figure 8, the data are collected in Table 2. The Tg obtained from the DSC analysis shows the same trend as the one obtained with DMTA.

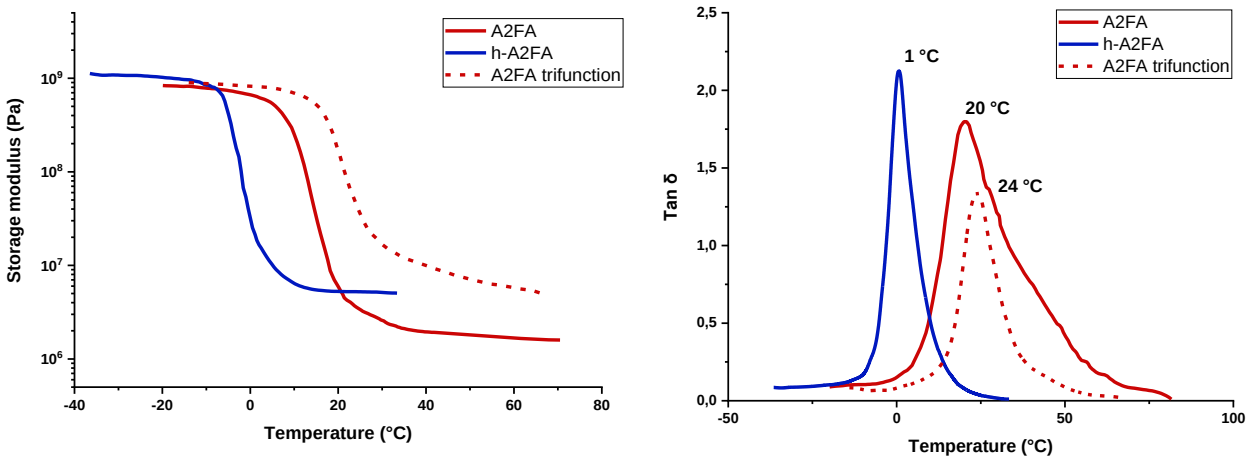

Figure 7: Storage modulus (left) and tan δ (right) as assessed by DMTA. The glass transition temperatures (Tg) of the crosslinked materials are defined as tan δ maximum. The analyzed samples formulations based on A2FA (Table 1, entry 1), h-A2FA (Table 1, entry 6), and A2FA trifunctional (Table 1, entry 2).

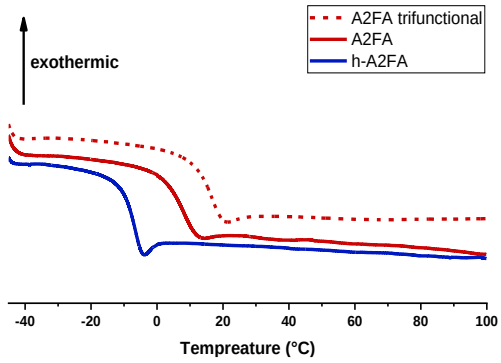

Figure 8: DSC thermograms of A2FA (Table 1, entry 1) and A2FA trifunctional (Table 1, entry 2) and h-A2FA (Table 1, entry 6) to highlight the differences in Tg of the main formulations. The thermograms ~~represented~~ show the second heating from -50 °C to 100 °C with an increase of 10 °C/min.

3.4 Copolymerization with the monofunctional ene-monomer h-EA1FA

The synthesized monofunctional ene-monomer, h-EA1FA, was added in the range between 5 to 15 wt-% to either A2FA or h-A2FA, with the aim to tailor the final Tg of the crosslinked networks, Table 1. The photorheology curves (Figure 9) show that the addition of the monofunctional monomer, within the investigated range, did not significantly influence the photocuring kinetics, but a linear lowering of the modulus upon curing was observed.

By increasing the co-monomer content, it was possible to observe a linear decrease of the Tg-values of the crosslinked films, measured as the maximum of tan δ curves (Figure 10), Table 2. This can be attributed to the decrease in cross-link density as an effect of the copolymerization with the A2FA. It was also shown that E' in the rubbery plateau (Figure 11) was decreased by increasing the amount of

monofunctional monomer in the photocurable formulation, confirming the decrease of the crosslinking density.

Table 2: Characteristics of the photocured networks as assessed by FT-IR analysis, DMTA and DSC analysis.

Entry	Formulation name	Conv.(1) (%)	T_g(2) (°C)	T_g(3) (°C)	E'(4) (MPa)	ν_c(5) (mmol/dm^3)
1	A2FA	86	20	6.0	2.08	258
2	A2FA (trifunctional)	99	24	15.0	6.38	781
3	A2FA+5% h-EA1FA	85	18	4.5	1.04	130
4	A2FA+10% h-EA1FA	85	17	2.5	5.65	71
5	A2FA+15%h-EA1FA	83	13	0.5	2.60	33
6	h-A2FA	99	1	-7.5	5.38	711
7	h-A2FA+5% h-EA1FA	100	0	-8.0	4.87	645
8	h-A2FA+10% h-EA1FA	100	-2	-9.5	3.75	500
9	h-A2FA+15% h-EA1FA	99	-5	-11.0	2.85	384

(1) Measured by FT-IR analysis.
(2) Measured by DMTA analysis as the maximum of tan δ peak.
(3) Measured by DSC analysis.
(4) Measured by DMTA analysis.
(5) Calculated by Equation 2.

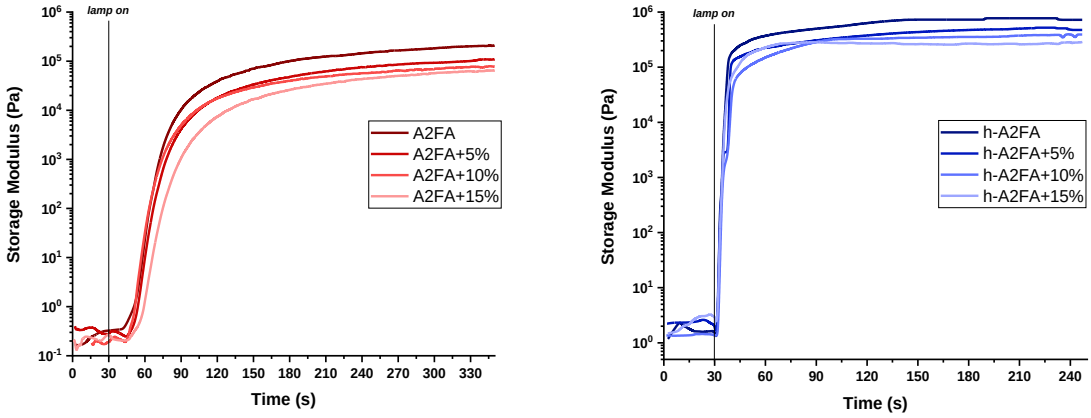

Figure 9: Results from photorheology of the analysed formulations of A2FA (left) (Table 2, entries 1, 3, 4, 5), and hA2FA (Table 2, entries 6, 7, 8, 9) (right). The comonomer was h-EA1FA.

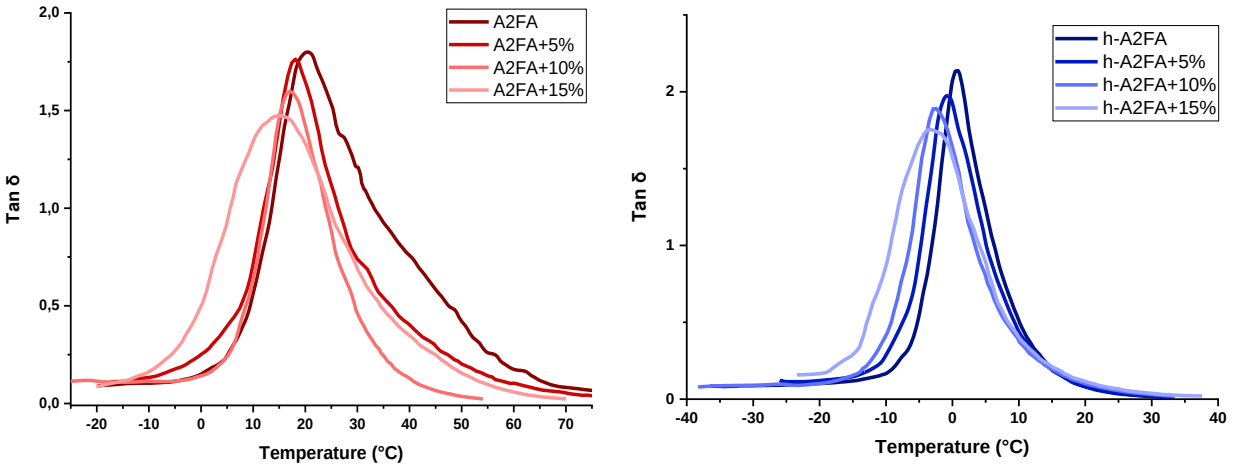

Figure 10: tan δ curves of A2FA samples on the left (Table 2, entries 1, 3, 4, 5) and of h-A2FA samples on the right (Table 2, entries 6, 7, 8, 9) with varying amounts of comonomer, h-EA1FA.

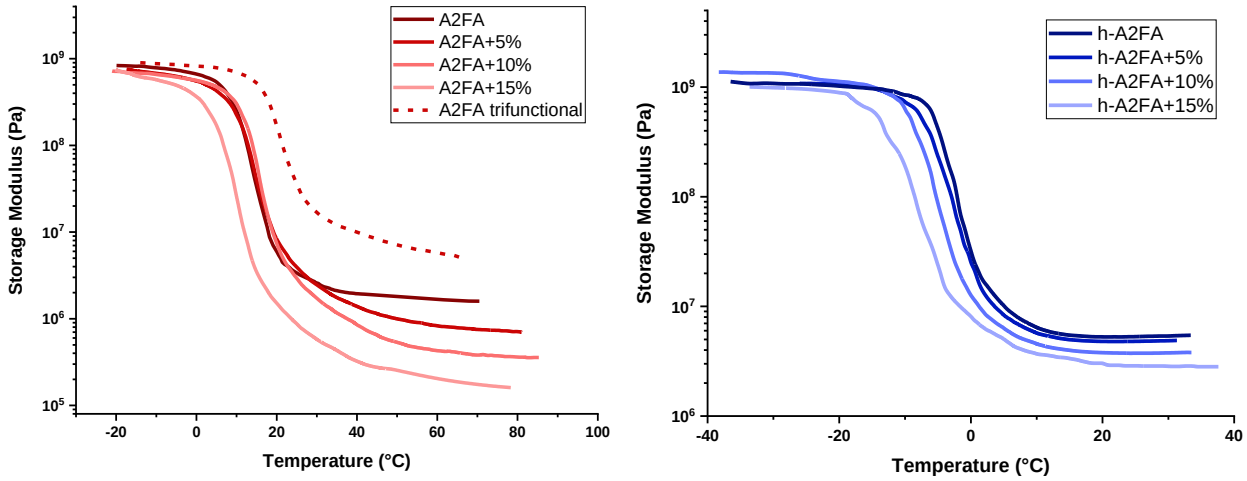

Figure 11: E' curves of A2FA (left) evaluated as a difunctional monomer (Table 2, entries 1, 3, 4, 5) (left) and for evaluation of A2FA as a trifunctional monomer (dashed line) (Table 2, entry 2). Evaluation of E' for h-A2FA (right) using different co-monomer concentrations. (Table 2, entries 6, 7, 8, 9).

3.5 Coating properties

Viscosity measurements were performed ~~on the investigated formulations before curing~~prior to cure. The formulations containing the ~~hydrogenated monomer~~monomer-A2FA showed a ~~much~~ lower viscosity ~~with respect the formulations containing the unsaturated FA~~than A2FA. This could be explained taking into account that the cinnamoyl double bond increase the rigidity of the molecule and the electron density by conjugation with the ~~ester group double bond~~carbonyl bond.~~, with a consequent higher viscosity~~

Contact angle against water ~~analysis with water~~was investigated ~~performed~~ on UV-~~C~~cured films showed similar wettability ~~behavior~~ for all ~~the~~ samples, with contact angles ~~between~~close to 67~~-66~~° ~~and 68°~~, ~~(see~~ Table 3~~)~~. The UV-cured coatings obtained by formulation 2, containing A2FA exploited as trifunctional monomer (~~see~~ Table 1), showed the highest contact angle, ~~reaching a value of~~ 75°. The higher contact angle value could be attributed to the higher amount of TRIS ~~monomer in the photocurable formulation.~~

All the UV-cured films showed ~~a~~ good hardness properties, between 6-H to 7 ~~H~~ as evaluated by pencil hardness. Adhesion was assessed by cross-hatch test and found to be best for the A2FA-based coatings.
~~The adhesion showed the best value for the A2FA coatings with 92 % of ahdesion.~~ The h-A2FA films showed a lower adhesion, attributed to the lower polarity and Tg. ~~the lower percentage of adhesion (55%). This is correlated to the Tg: the h-A2FA film was softer (Tg around 0 °C) than A2FA films (Tg around 20 °C) showing a lower level of adhesion.~~

Table 3: Coating properties of the analyzed films.~~measured properties for the different UV-cured formulations.~~

Entry	Formulation name	Contact angle (°)	Viscosity (Pa s)	Pencil hardness	Adhesion (%)
1	A2FA	66 ± 1	0.21~~0~~ ± 0.05~~0~~	7 H	82
2	A2FA (trifunctional)	75 ± 1		7 H	92
3	A2FA+5% h-EA1FA	68 ± 1		7 H	87
4	A2FA+10% h-EA1FA	68 ± 2		7 H	88
5	A2FA+15%h-EA1FA	68 ± 2		6 H	90
6	h-A2FA	66 ± 2	0.04~~7~~5 ± 0.00~~0~~15	7 H	55
7	h-A2FA+5% h-EA1FA	67 ± 2		7 H	60
8	h-A2FA+10% h-EA1FA	68 ± 2		7 H	59
9	h-A2FA+15% h-EA1FA	68 ± 1		6 H	65

4. CONCLUSIONS

Allyl-functionalized ferulic acid (FA) based monomers were synthesized and their reactivity towards thiol-ene photopolymerization investigated, using trimethylolpropane tris(3-mercaptopropionate) (TRIS) as thiol monomer in 1:1 molar ratio, –SH to ene functionalities. Photorheology analysis showed higher reactivity of the hydrogenated allyl-FA (h-2AFA) towards TRIS than the A2FA monomer, which showed an induction time attributable to the competitive absorbance with the photoinitiator. When the cinnamoyl-double bond is removed by hydrogenation, the h-2AFA monomer's absorption in the UV region is shifted to shorter wavelengths and no more UV-absorption competition occurs why a faster photocuring polymerization without any induction time is observed. The FT-IR analysis was in agreement with the photorheology after 2 minutes of irradiation. The A2FA monomer showed a high degree of unreacted double bond when considered difunctional. An almost complete conversion of C=C double bond was achieved by increasing the thiol content in the photocurable formulation considering the A2FA monomer as a trifunctional ene-monomer. The thermomechanical properties of crosslinked films were fully characterized by DMTA and DSC analyses. The modulus recorded for the crosslinked films obtained by A2FA monomer, considered as a bifunctional ene-monomer, reached lower value than the modulus registered for the crosslinked films obtained by the h-A2FA monomer. This agrees with the photo-rheology data. The E' evaluated

for the crosslinked films obtained by considering the monomer A2FA as trifunctional was the highest. The data was in good agreement with the higher conversion calculated in the FTIR analysis when stochiometric amount of thiol was added with respect to A2FA monomer as a trifunctional ene-monomer, therefore considering the cinnamoyl double bond reactive towards thiol-ene reaction as well as the allyl double bond. Finally, the synthesized monofunctional ene-monomer, h-EA1FA, was added in the range between 5 to 15 wt-% in both A2FA- and h-A2FA-monomers, with the aim to tailor the final Tg of the crosslinked networks. By increasing the co-monomer content, it was possible to observe a linear decrease of the Tg values of crosslinked films, measured as the maximum of tanδ curves.

Contact angle measurements ~~with~~against water ~~performed on UV-Cured films~~ showed similar wettability on all films based on h-A2FA, while ~~the the UV-cured coating obtained by formulation 2, containing~~ A2FA ~~–~~containing film exhibited a higher contact angle. All coatings had acceptable adhesion. ~~exploited as trifunctional monomer, showed a higher contact angle value. Coating adhesion was very good for A2FA UV-cured formulations and in general the adhesion value decrease by decreasing the Tg values of the cured films.~~

In conclusion, this work demonstrates the feasibility of using ~~Ferulic~~ ferulic acid as a green starting monomer for developing UV-curable coatings, with the possibility to modulate the final Tg of crosslinked networks.

REFERENCES

[1] L. Y. Ljungberg, “Materials selection and design for development of sustainable products,” *Mater. Des.*, vol. 28, no. 2, pp. 466–479, 2007.

[2] T. F. Garrison, A. Murawski, and R. L. Quirino, “Bio-based polymers with potential for biodegradability,” *Polymers (Basel).*, vol. 8, no. 7, pp. 1–22, 2016.

[3] A. Gandini, “The irruption of polymers from renewable resources on the scene of macromolecular science and technology,” *Green Chem.*, vol. 13, no. 5, pp. 1061–1083, 2011.

[4] A. Gandini, “Polymers from renewable resources: A challenge for the future of macromolecular materials,” *Macromolecules*, vol. 41, no. 24, pp. 9491–9504, 2008.

[5] A. C. Fonseca, M. S. Lima, A. F. Sousa, A. J. Silvestre, J. F. J. Coelho, and A. C. Serra, “Cinnamic acid derivatives as promising building blocks for advanced polymers: Synthesis, properties and applications,” *Polym. Chem.*, vol. 10, no. 14, pp. 1696–1723, 2019.

[6] J. P. N. Rosazza, Z. Huang, L. Dostal, T. Volm, and B. Rousseau, “Biocatalytic transformations of ferulic acid: An abundant aromatic natural product,” *J. Ind. Microbiol.*, vol. 15, no. 6, pp. 472–479, 1995.

[7] W. Boerjan, J. Ralph, and M. Baucher, “Lignin Biosynthesis,” *Annu. Rev. Plant Biol.*, vol. 54, no. 1, pp. 519–546, 2003.

[8] F. Pion, P. H. Ducrot, and F. Allais, “Renewable alternating aliphatic-aromatic copolyesters derived from biobased ferulic acid, diols, and diacids: Sustainable polymers with tunable thermal properties,” *Macromol. Chem. Phys.*, vol. 215, no. 5, pp. 431–439, 2014.

[9] A. Bento-Silva, M. C. Vaz Patto, and M. do Rosário Bronze, “Relevance, structure and analysis of ferulic acid in maize cell walls,” *Food Chem.*, vol. 246, no. April 2017, pp. 360–378, 2018.

[10] D. M. de Oliveira, A. Finger-Teixeira, T. Rodrigues Mota, V. H. Salvador, F. C. Moreira-Vilar, H. B. Correa Molinari, R. A. Craig Mitchell, R. Marchiosi, O. Ferrrarese-Filho, and W. dos Santos, “Ferulic acid: a key component in grass lignocellulose recalcitrance to hydrolysis,” *Plant Biotechnol. J.*, vol. 13, no. 9, pp. 1224–1232, 2015.

[11] N. Kumar and V. Pruthi, “Potential applications of ferulic acid from natural sources,” *Biotechnol. Reports*, vol. 4, no. 1, pp. 86–93, 2014.

[12] D. D. Peres, F. D. Sarruf, C. A. de Oliveira, M. V. R. Velasco, and A. R. Baby, “Ferulic acid photoprotective properties in association with UV filters: multifunctional sunscreen with

improved SPF and UVA-PF," *J. Photochem. Photobiol. B Biol.*, vol. 185, pp. 46–49, 2018.
[13] L. Mialon, A. G. Pemba, and S. A. Miller, "Biorenewable polyethylene terephthalate mimics derived from lignin and acetic acid," *Green Chem.*, vol. 12, no. 10, pp. 1704–1706, 2010.
[14] A. Llevot, E. Grau, S. Carlotti, S. Grelier, and H. Cramail, "From Lignin-derived Aromatic Compounds to Novel Biobased Polymers," *Macromol. Rapid Commun.*, vol. 37, no. 1, pp. 9–28, 2016.
[15] A. B. Scranton, C. N. Bowman, and R. W. Peiffer, *Photopolymerization: fundamentals and applications*. ACS Publications, 1997.
[16] S. K. Rajaraman, W. A. Mowers, and J. V. Crivello, "Novel hybrid monomers bearing cycloaliphatic epoxy and 1-propenyl ether groups," *Macromolecules*, vol. 32, no. 1, pp. 36–47, 1999.
[17] R. S. Davidson, *Exploring the science, technology and applications of UV and EB curing*. Sita Technology, 1999.
[18] N. B. Cramer and C. N. Bowman, "Kinetics of thiol-ene and thiol-acrylate photopolymerizations with real-time Fourier transform infrared," *J. Polym. Sci. Part A Polym. Chem.*, vol. 39, no. 19, pp. 3311–3319, 2001.
[19] Y. Yagci, "Photoinitiated cationic polymerization of unconventional monomers," *Macromol. Symp.*, vol. 240, pp. 93–101, 2006.
[20] M. Sangermano, "Advances in cationic photopolymerization," *Pure Appl. Chem.*, vol. 84, no. 10, pp. 2089–2101, 2012.
[21] M. Sangermano, N. Razza, and J. V. Crivello, "Cationic UV-curing: Technology and applications," *Macromol. Mater. Eng.*, vol. 299, no. 7, pp. 775–793, 2014.
[22] M. Sangermano, I. Roppolo, and M. Messori, "UV-cured functional coatings," *Photocured Mater.*, no. 13, p. 121, 2014.
[23] M. Sangermano, "Recent advances in cationic photopolymerization," *J. Photopolym. Sci. Technol.*, vol. 32, no. 2, pp. 233–236, 2019.
[24] M. Claudino, M. Johansson, and M. Jonsson, "Thiol-ene coupling of 1,2-disubstituted alkene monomers: The kinetic effect of cis/trans-isomer structures," *Eur. Polym. J.*, vol. 46, no. 12, pp. 2321–2332, 2010.
[25] O. Türünç, M. Firdaus, G. Klein, and M. A. R. Meier, "Fatty acid derived renewable polyamides via thiol-ene additions," *Green Chem.*, vol. 14, no. 9, pp. 2577–2583, 2012.
[26] M. Claudino, J. M. Mathevet, M. Jonsson, and M. Johansson, "Bringing d-limonene to the scene of bio-based thermoset coatings via free-radical thiol-ene chemistry: Macromonomer synthesis, UV-curing and thermo-mechanical characterization," *Polym. Chem.*, vol. 5, no. 9, pp. 3245–3260, 2014.
[27] M. Claudino, I. Van Der Meulen, S. Trey, M. Jonsson, A. Heise, and M. Johansson, "Photoinduced thiol-ene crosslinking of globalideε-caprolactone copolymers: Curing performance and resulting thermoset properties," *J. Polym. Sci. Part A Polym. Chem.*, vol. 50, no. 1, pp. 16–24, 2012.
[28] A. Stamm, M. Tengdelius, B. Schmidt, J. Engström, P. O. Sirèn, L. Fogelstöm, and E. Malmström "Chemo-enzymatic pathways toward pinene-based renewable materials," *Green Chem.*, vol. 21, no. 10, pp. 2720–2731, 2019.
[29] M. Fache, E. Darroman, V. Besse, R. Auvergne, S. Caillol, and B. Boutevin, "Vanillin, a promising biobased building-block for monomer synthesis," *Green Chem.*, vol. 16, no. 4, pp. 1987–1998, 2014.
[30] T. M. Roper, T. Y. Lee, C. A. Guymon, and C. E. Hoyle, "In situ characterization of photopolymerizable systems using a thin-film calorimeter," *Macromolecules*, vol. 38, no. 24, pp. 10109–10116, 2005.
[31] S. K. Reddy, O. Okay, and C. N. Bowman, "Network development in mixed step-chain growth thiol-vinyl photopolymerizations," *Macromolecules*, vol. 39, no. 25, pp. 8832–8843, 2006.

[32] S. K. Reddy, N. B. Cramer, and C. N. Bowman, “Thiol-vinyl mechanisms. 2. Kinetic modeling of ternary thiol-vinyl photopolymerizations,” *Macromolecules*, vol. 39, no. 10, pp. 3681–3687, 2006.
[33] M. Shibata, K. Sugane, and Y. Yanagisawa, “Biobased polymer networks by the thiol-ene photopolymerization of allylated p-coumaric and caffeic acids,” *Polym. J.*, vol. 51, no. 5, pp. 461–470, 2019.
[34] M. Jawerth, M. Lawoko, S. Lundmark, C. Perez-Berumen, and M. Johansson, “Allylation of a lignin model phenol: a highly selective reaction under benign conditions towards a new thermoset resin platform,” *RSC Adv.*, vol. 6, no. 98, pp. 96281–96288, 2016.
[35] BASF SE, “High lights! Radiation curing with resins and photoinitiators for industrial coatings and graphic arts: Laromer®, Irgacure®, Lucirin®, Darocur®.” [Online]. Available: https://www.dispersions-pigments.basf.com/portal/load/fid620253/low_EDC_2711_e_BR_Strahlung.pdf. [Accessed: 26-Jun-2020].